SCIENTIFIC REPORTS

OPEN

SUBJECT AREAS:
POPULATION DYNAMICS
BIOGEOGRAPHY
FISHERIES

Received
13 January 2014

Accepted
26 August 2014

Published
16 September 2014

Correspondence and requests for materials should be addressed to L.J.H. (tiger02j@hotmail.com)

* These authors contributed equally to this work.

Demographic response of cutlassfish (*Trichiurus japonicus and T. nanhaiensis*) to fluctuating palaeo-climate and regional oceanographic conditions in the China seas

Lijun He[1,2], Aibing Zhang[3]*, David Weese[4]*, Shengfa Li[2]*, Jiansheng Li[2] & Jing Zhang[1]

[1]State Key Laboratory of Estuarine and Coastal Research, East China Normal University, Shanghai, 200062, P. R. China, [2]East China Sea Fisheries Research Institute, Chinese Academy of Fishery Sciences, Shanghai, 200090, P. R. China, [3]College of Life Sciences, Capital Normal University, Beijing, 100048, P. R. China, [4]Department of Biological and Environmental Sciences, Georgia College & State University, Milledgeville, GA 31061, USA.

Glacial cycles of the Quaternary have heavily influenced the demographic history of various species. To test the evolutionary impact of palaeo-geologic and climatic events on the demographic history of marine taxa from the coastal Western Pacific, we investigated the population structure and demographic history of two economically important fish (*Trichiurus japonicus* and *T. nanhaiensis*) that inhabit the continental shelves of the East China and northern South China Seas using the mitochondrial cytochrome b sequences and Bayesian Skyline Plot analyses. A molecular rate of 2.03% per million years, calibrated to the earliest flooding of the East China Sea shelf (70–140 kya), revealed a strong correlation between population sizes and primary production. Furthermore, comparison of the demographic history of *T. japonicus* populations from the East China and South China Seas provided evidence of the postglacial development of the Changjiang (Yangtze River) Delta. In the South China Sea, interspecific comparisons between *T. japonicus* and *T. nanhaiensis* indicated possible evolutionary responses to changes in palaeo-productivity that were influenced by East Asian winter monsoons. This study not only provides insight into the demographic history of cutlassfish but also reveals potential clues regarding the historic productivity and regional oceanographic conditions of the Western Pacific marginal seas.

Glacial cycles and the consequent sea-level fluctuations of the Quaternary epoch greatly influenced the spatial distribution and population dynamics of a number of terrestrial[1–3], freshwater[4,5] and marine species[6–8]. This was particularly true for marine organisms of oceans and marginal seas[9–11]. The advancing terrestrial ice sheets and falling sea level during glacial periods exposed shallow coastal continental shelves[12–14], greatly reducing habitat availability for many marine taxa. However, rising sea levels during the interglacial periods inundated continental shelves and enlarged marginal seas on a global scale[15]. These cyclic changes in habitat availability likely led to repeated range expansions and contractions, influencing the population dynamics of various taxa[16,17].

The China seas, including the South China Sea (SCS), East China Sea (ECS), Yellow Sea (YS) and Bohai Sea (BH), are relatively young (*i.e.*, <30 million years [myr]) marginal seas of the Western Pacific Ocean[18] (Fig. 1). The Bohai, Yellow and East China Seas share a wide and shallow continental shelf, whereas the South China Sea forms a deep sea basin with a narrow continental shelf in the north and the wide Sunda Shelf in the southwest. These marginal seas are supplied with high levels of terrigenous nutrients from the Asian continent through river run-off, which has led to high primary productivity and increased fish production[19]. During the Pleistocene, sea-level fluctuations would have repeatedly exposed and inundated these shallow marginal seas, dramatically changing nutrient input and habitat availability. For example, some recent studies have revealed similar patterns of population expansions for a number of marine taxa in response to Pleistocene sea-level fluctuations in the China seas[10,20–22]. Furthermore, the Yellow-Bohai, East China and South China Seas have been identified as large

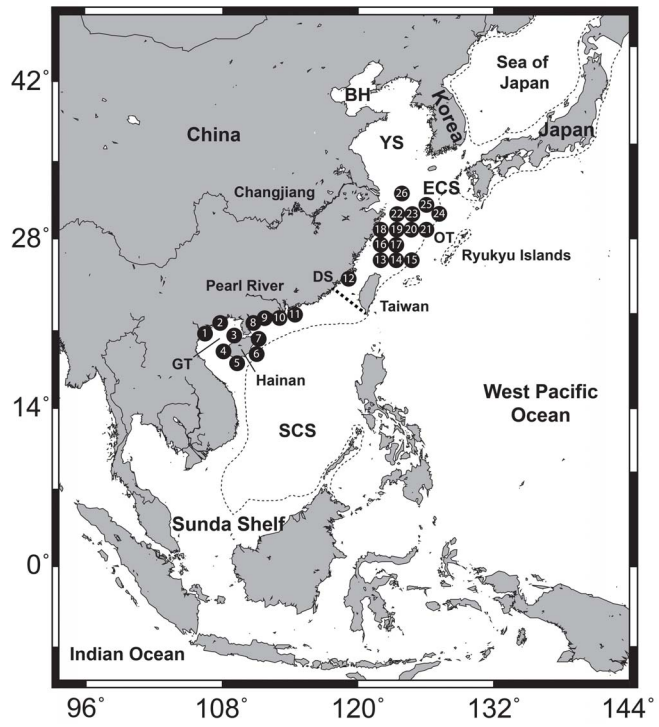

Figure 1 | Map of the East China and northern South China Seas from which individuals of *Trichiurus japonicus* and *T. nanhaiensis* were sampled for this study. Individual sampling sites are listed in Table 1. The shoreline of the LGM (−130 m) is indicated by thin dashed line and the boundary of the East China Sea and South China Sea is indicated by thick dashed line. BH = Bohai Sea, YS = Yellow Sea, ECS = East China Sea, SCS = South China Sea, OT = Okinawa Trough, DS = Dongshan, GT = Gulf of Tonkin. Map was created in software Generic Mapping Tools (GMT v3.1.1; http://gmt.soest.hawaii.edu/).

marine ecosystems (LMEs) that have global importance, based on their distinct bathymetry, hydrography, productivity and trophic relationships[23], and the different oceanographic conditions of these LMEs are expected to have influenced the evolutionary histories of regional populations. However, comparative studies investigating the dynamic responses of different marine taxa to endemic oceanographic conditions among these LMEs are lacking. Influenced by past geologic and climatic events, understanding the demographic history of regional populations of marine organisms from the China seas may provide a framework for elucidating the historic climatic and oceanographic conditions of the Western Pacific Ocean.

The Trichiuridae (cutlassfish or hairtails) are an economically important group of benthic fish that inhabit the continental shelves and shallow seas (20–200 m) of tropical and temperate waters[24], with over 80% of global cutlassfish catch production originating from the China seas[25]. Furthermore, cutlassfish are the most important commercial marine fish species in East Asia, accounting for 8.5–18.3% of the total annual fishing catch in the China seas between 1950 and 2000[26]. Given these pressures, it is not surprising that the overexploitation of cutlassfish in recent years has led to a dramatic decrease in catch production and population size[27]. Additionally, increased fishing pressures have led to reductions in average body size and increases in maturation rates[28]. Given the glacial cycles mentioned above and these recent anthropogenic pressures, cutlassfish in the Western Pacific region are predicted to have a complex and dynamic demographic history.

The demographic history of populations can often be revealed by analysing the genetic variation using coalescent-based statistical methodologies, such as mismatch distribution[29] and Bayesian Skyline Plot (BSP) analyses[30]. For example, these types of analyses have revealed repeated periods of population expansions and contractions due to glacial cycles, sea-level fluctuations and anthropogenic pressures for a number of marine taxa such as mitten crabs (*Eriocheir sensu stricto*) in the East Asian marginal seas[31], North Pacific herring (*Clupea pallasii*)[8] and Antarctic fur seals (*Arctocephalus gazelle*)[32]. In this study, the genetic variation and demographic history of two cutlassfish species, *T. japonicus* from the northern South China Sea and East China Sea and *T. nanhaiensis* from the northern South China Sea, were investigated via sequence analyses of the mitochondrial cytochrome b (*Cyt b*) gene and via BSP. Specifically, we attempted to investigate the evolutionary influences of past climatic events and regional oceanographic conditions on the demographic histories of marine organisms, including *T. japonicus* and *T. nanhaiensis*, in two West Pacific marginal seas, the northern South China Sea and the East China Sea.

Results

Population genetic analyses. A total of 761 cutlassfish were collected from 26 sampling sites in the East China Sea and northern South China Sea (Fig. 1). Direct sequencing of the *Cyt b* gene resulted in 509 and 252 sequences belonging to *T. japonicus* (400, East China Sea; 109, South China Sea) and *T. nanhaiensis* (South China Sea), respectively. From these, 239 *T. japonicus* and 74 *T. nanhaiensis* unique *Cyt b* haplotypes were identified and deposited into GenBank under the accession numbers KF551253–KF551565. Specific sample sizes and numbers of haplotypes recovered for each species from each locality are summarised in Tables 1 and 2. Estimates of haplotype diversity (h) and nucleotide diversity (π) for *T. japonicus* were mostly consistent among sampling sites and geographic populations (Table 1). However, high haplotype diversities and low nucleotide diversities were observed for *T. nanhaiensis* at each locality, indicating recent population expansions (Table 1).

A star-like network radiating from a central haplotype was recovered from the median-joining network analyses of *T. japonicus Cyt b* sequences (Fig. 2a). Within the network, haplotypes sampled from the East China Sea and northern South China Sea were evenly distributed. Network analyses of *T. nanhaiensis Cyt b* sequences from the northern South China Sea produced one network with two divergent clusters (I and II) distinguished by nine substitutions (net distance, 0.989%; Fig. 2b). The majority (243) of *T. nanhaiensis Cyt b* sequences belonged to cluster I and exhibited a diffuse network pattern deriving from three dominant haplotypes. The remaining nine sequences belonged to cluster II. No obvious geographic structure was observed between clusters I and II.

Molecular rate calibration. Using the equation $\mu = \tau/(2mt)$ and the flooding of the East China Sea shelf 70–140 kya as a calibration point, a mutation rate of 2.03% (1.35–2.7%) per myr was inferred. If the earliest population expansion of cutlassfish in the East China Sea induced by the postglacial high sea levels of $<$22 kya was used as a calibration point, a substitution rate of over 9.7% per myr could be inferred, which is approaching the maximum substitution rate estimated for the mitochondrial control region of fish[33]. Because the substitution rate of *Cyt b* is much slower than the mitochondrial control region in fishes[34], the calibration point of the Last Interglacial sea level highstand (70–140 kya) used here appears to be more appropriate. However, given the uncertainty of rate estimates, the maximum (*i.e.*, 2.7% per myr) and minimum (*i.e.*, 1.35% per myr) estimated rates (bracketed values) were also used in the BSP inference analyses below.

Population dynamics. The pairwise mismatch distributions for *T. japonicus* as a whole and the two geographic groups of *T. japonicus* were unimodal (Fig. 3a, b). Additionally, no significant deviation was found between any of the observed distributions and expected

Table 1 | Sampling locations and indices of genetic diversity of *T. japonicus* and *T. nanhaiensis* collected from the South and East China Seas. Letters indicate variables: *n*, sample size; *nh*, haplotype number; *h*, haplotype diversity; π, nucleotide diversity

		Trichiurus japonicus				*Trichiurus nanhaiensis*			
ID	Localities	*n*	*nh*	*h*	π (%)	*n*	*nh*	*h*	π (%)
					South China Sea				
1	Haifang, Vietnam	-	-	-	-	32	17	0.8831	0.2558
2	Beihai, Guangxi, China	1	1	1.0000	0	9	6	0.8889	0.3917
3	Baimajing, Hainan, China	28	25	0.9894	0.6420	-	-	-	-
4	Dongfang, Hainan, China	11	9	0.9455	0.5629	45	19	0.8717	0.2431
5	Sanya, Hainan, China	39	28	0.9825	0.5309	-	-	-	-
6	Wenchang, Hainan, china	16	12	0.9417	0.5703	44	22	0.8901	0.2377
7	Tongguling, Hainan, China	4	4	1.0000	0.4486	41	15	0.8061	0.2272
8	Zhanjiang, Guangdong, China	-	-	-	-	20	8	0.7789	0.2084
9	Yangjiang, Guangdong, China	-	-	-	-	39	20	0.9015	0.2523
10	Taishan, Guangdong, China	4	4	1.0000	0.7684	19	8	0.8655	0.1519
11	Dongguan, Guangdong, China	6	6	1.0000	0.4663	3	3	1.0000	0.2983
	Total	109	73	0.9849	0.5745	252	74	0.8727	0.2343
					East China Sea				
12	Xiamen, Fujian, China	4	4	1.0000	0.5088	-	-	-	-
13	D14	14	12	0.9780	0.6410	-	-	-	-
14	D18	14	13	0.9890	0.5690	-	-	-	-
15	D19	14	11	0.9341	0.5030	-	-	-	-
16	D04	26	22	0.9785	0.5430	-	-	-	-
17	D05	24	22	0.9928	0.7074	-	-	-	-
18	D01	48	32	0.9450	0.4948	-	-	-	-
19	D03	15	13	0.9714	0.5083	-	-	-	-
20	C20	54	36	0.9651	0.5118	-	-	-	-
21	C21	18	13	0.9281	0.5011	-	-	-	-
22	C12	44	37	0.9926	0.5817	-	-	-	-
23	C13	26	24	0.9938	0.5326	-	-	-	-
24	C16	38	34	0.9929	0.5836	-	-	-	-
25	C07	31	24	0.9634	0.6028	-	-	-	-
26	C01	30	21	0.9557	0.5005	-	-	-	-
	Total	400	193	0.9726	0.5409	-	-	-	-

distributions of haplotypes based on the sudden expansion model (Table 2), indicating recent population expansions. Furthermore, neutrality tests (Tajima's D and Fu's F_s) revealed significant negative values for all species and geographic groups (Table 2). Taken together, these results indicate recent population expansion in both *T. japonicus* and *T. nanhaiensis* and in the two geographic groups of *T. japonicus*.

Based on extended BSP analyses, the number of groups of coalescent intervals was inferred from each data set with a mean of 2.436 with 95% credible set {1, 4} for *T. japonicus*, 2.051{1, 4} for the East China Sea population of *T. japonicus*, 1.598{1, 3} for the South China Sea population of *T. japonicus* and 1.612 {1, 3} for *T. nanhaiensis*. These statistics strongly support a complex population demographic model (*e.g.*, BSP) over a single constant population size model (1-group model).

Population size fluctuations through time were further compared using BSP among species and geographic groups (Figs. 4, 5), and the partitioning of *Cyt b* sequences between 3 codon positions neither improved the resolution nor changed the results (data not shown). For *T. japonicus* as a whole, BSP revealed two episodes of population growths (Fig. 4). The first episode of rapid population growth occurred 45–105 kya [30–70 kya, 2.7% per myr; 60–140 kya, 1.35% per myr] and was followed by a reduction in population size 22.5–37.5 kya [15–25 kya, 2.7% per myr; 30–50 kya, 1.35% per myr] that coincided with the Last Glaciation Maximum (LGM). Following the LGM and continuing to the present, *T. japonicus* experienced a second and more rapid episode of population growth 0–22.5 kya [0–15 kya, 2.7% per myr; 0–30 kya, 1.35% per myr]. The current population size of *T. japonicus* appears to be two orders of magnitude larger than it was at the time of coalescence 304 (202.7–405) kya (Fig. 4).

Despite showing little genetic differentiation or population structure, *T. japonicus* sampled from the East China Sea and northern South China Sea exhibit distinct demographic histories. Similar to the species as a whole, BSP analysis revealed two episodes of population growth for *T. japonicus* from the East China Sea (Fig. 4). However, *T. japonicus* from the northern South China Sea only exhibited a single period of population growth occurring 45–

Table 2 | Results of dynamic tests and molecular clock analyses for *T. japonicus* and *T. nanhaiensis* from the South and East China Seas. Letters indicate variables and abbreviations: *n*, sample size; *nh*, haplotype number; *h*, haplotype diversity; π, nucleotide diversity; SSD = sum of square deviations between the observed and expected mismatch, τ = mutational time scale. *$P < 0.05$, ** $P < 0.001$

Species	Group	*n*	*nh*	*h*	π (%)	Tajima's *D*	Fu's F_s	SSD/P	τ	Coalescent time (kyr, 2.03% per myr)
T. japonicus	Total	509	239	0.9741	0.55	−2.3359**	−24.4302**	0.0007/0.614	4.344	303.98 (178.86–455.07)
	South China Sea	109	73	0.9849	0.57	−2.1519**	−25.0221**	0.0017/0.541	4.984	265.53 (147.20–398.72)
	East China Sea	400	193	0.9726	0.54	−2.331**	−24.5337**	0.0007/0.659	4.289	299.22 (174–452.60)
T. nanhaiensis	Total	252	74	0.8727	0.23	−2.3928**	−26.3877**	0.0021/0.07	1.930	291.11 (145.76–457.52)

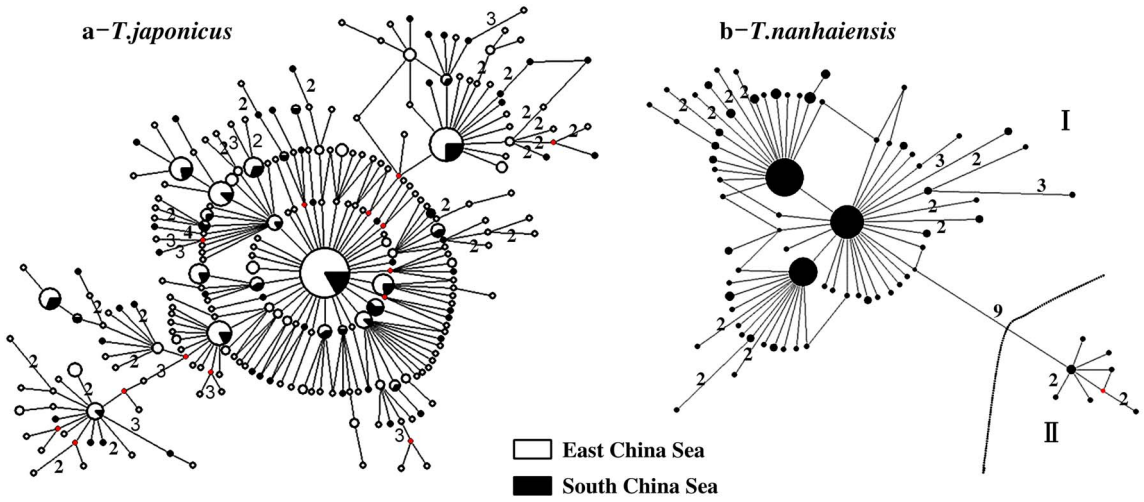

Figure 2 | Evolutionary networks depicting relationships among *Cyt b* haplotypes recovered from *T. japonicus* and *T. nanhaiensis*. Geographic information for haplotypes is distinguished using white (East China Sea) and black (South China Sea). The sizes of circles are proportional to the frequency at which specific haplotypes were recovered. Numbers indicate mutational differences of two or more substitutions. For each network, red dots represent unsampled (missing) haplotypes.

105 kya [30–70 kya, 2.7% per myr; 60–140 kya, 1.35% per myr], similar to that observed in the East China Sea (Fig. 4). This period of population growth (45–105 kya) resulted in a 10-fold increase in population size for both the East China Sea and northern South China Sea populations relative to those at the times of coalescence for these populations. However, in the northern South China Sea, this growth continued, peaked during the LGM (22–30 kya) and has since undergone a steady decline (Fig. 4, Fig. 5). As a result, the present population size of *T. japonicus* in the East China Sea is ca. 20 times larger than that in the northern South China Sea (Fig. 4). Haplotypes of *T. japonicus* from the northern South China Sea exhibit a younger coalescent time of 266 kya [177–354 kya] compared with that of 299.3 kya [199.5–399 kya] for haplotypes of *T. japonicus* from the East China Sea.

T. nanhaiensis from the northern South China Sea appears to have responded differently to the climatic dynamics of the area (Fig. 5). BSP revealed a steady population decline 37.5–165 kya [25–110 kya, 2.7% per myr; 50–220 kya, 1.35% per myr] followed by a rapid population expansion (15–37.5) [10–25 kya, 2.7% per myr; 20–50 kya, 1.35% per myr), with an estimated 100-fold increase in the maximum effective population size. However, beginning ~15 kya [10–20 kya] and continuing to the present, *T. nanhaiensis* has been undergoing a second bottleneck event, and its population has been reduced to a size similar to that of the northern South China Sea

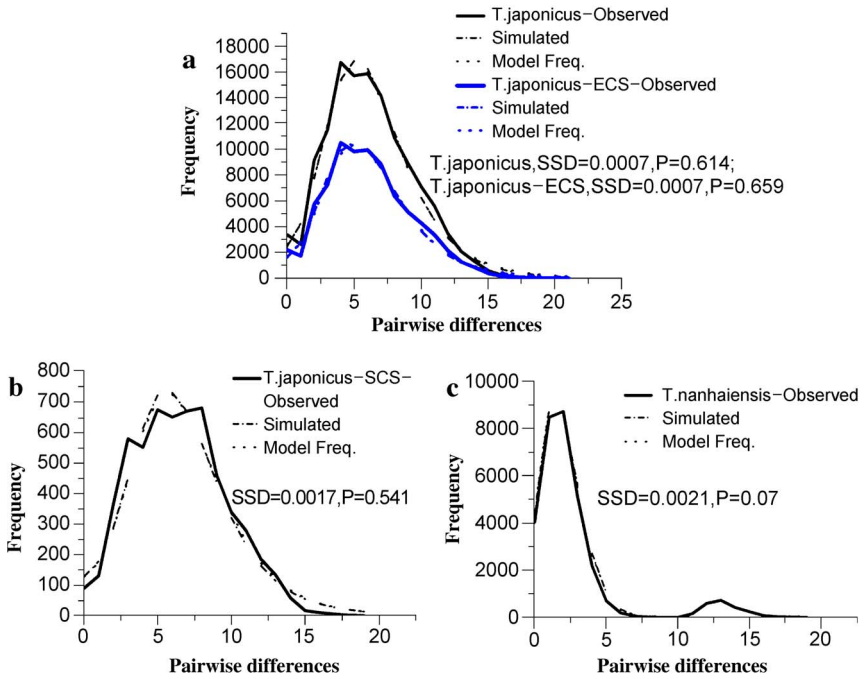

Figure 3 | Mismatch distribution analyses of *T. japonicus* and *T. nanhaiensis* in the China seas. (a) *T. japonicus and T. japonicus* population of the East China Sea; (b) *T. japonicus* population of the South China Sea and (c) *T. nanhaiensis* population of the South China Sea.

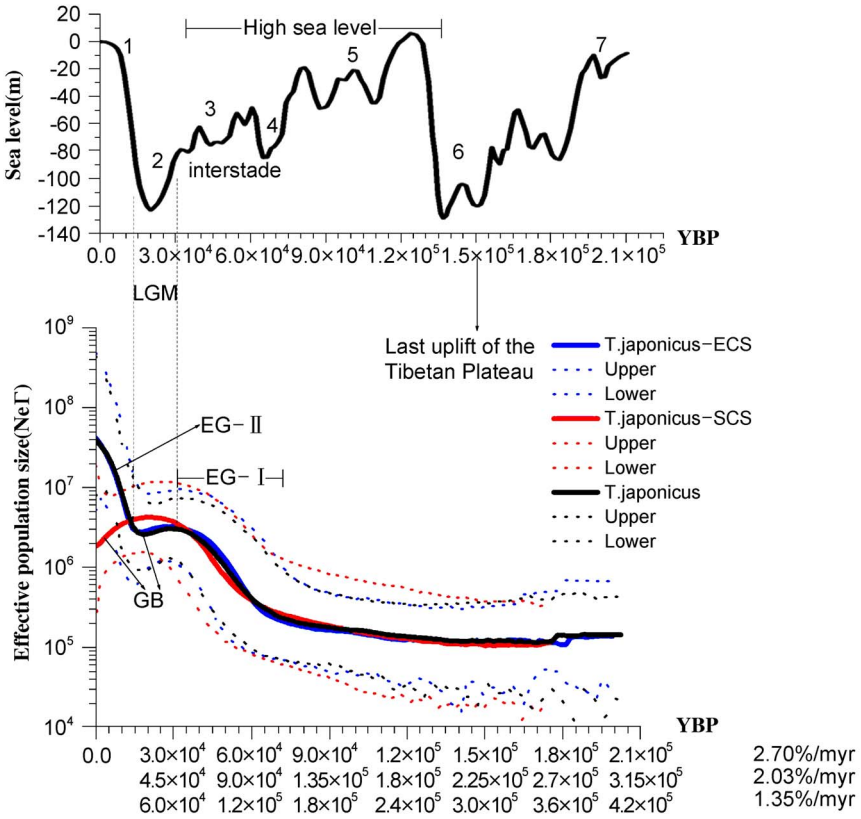

Figure 4 | Sea-level changes and demographic history of *T. japonicus* over the past 315 kya (2.03% per myr). Top panel: Sea level fluctuations through marine oxygen isotope stages (MIS) are redrawn from Waelbroeck *et al.*[83]. Bottom panel: BSPs of *T. japonicus*, including both of the geographic groups (East China Sea and northern South China Sea). Solid lines indicate the median estimate, and dotted lines indicate 95% credibility intervals. Expansion growth (EG) and genetic bottleneck (GB) through time (years before present, YBP) are also indicated.

population of *T. japonicus* (Fig. 5). Haplotypes of *T. nanhaiensis* in the northern South China Sea were estimated to have coalesced 291 kya [194.1–388.2 kya].

Discussion

Because substitution rates of the mitochondrial *Cyt b* gene in fish appear to be variable[35–39] and time-dependent[40–44], the present study used two recent historical events to calibrate a molecular clock for *Trichiurus* (Supplementary information S1). Despite some uncertainty, the molecular rate of 2.03 (1.35–2.7)% per myr estimated here provides an approximate timescale for better understanding the influence of late Pleistocene climatic events on the evolution and ecology of marine organisms.

As top predators, the population abundance of marine fish has been considered a good indicator of primary productivity[45,46], which appears to hold true for the population demographic history of *T. japonicus* and *T. nanhaiensis* in the China seas. The differences between present-day (t = 0) estimated effective population sizes for intraspecific geographic groups (East China Sea vs. northern South China Sea) of *T. japonicus* or interspecific geographic groups (the East China Sea population of *T. japonicus* vs. the northern South China Sea population of *T. nanhaiensis*) reach an order of magnitude (Figs. 4, 5), suggesting that the East China Sea supports ca. 20 times more cutlassfish than the northern South China Sea. These differences in the estimated regional effective population sizes are consistent with cutlassfish surveys in the China seas, where over 80% of the annual catch of cutlassfish originates from the East China Sea[26].

Several factors may have led to the higher effective population size and biomass of *T. japonicus* in the East China Sea than in the northern South China Sea. First, as mentioned above, cutlassfish are benthic fishes that inhabit the photic zone above continental shelves at a depth of 20–200 m[24,26]. In this context, the East China Sea has a much wider continental shelf (540,000 km^2), providing a greater area of suitable habitat than the narrower and deeper northern slope of the South China Sea (370,000 km^2)[47]. Second, the East China Sea possesses a higher average annual primary productivity (609.65 gC m^{-2}a^{-1}) than does the northern South China Sea (100.09 gC m^{-2}a^{-1})[48], directly supporting a higher biomass of zooplankton and fish[19,49]. Finally, the lower species diversity in the East China Sea (4,167 species), compared with that in the South China Sea (5,613 species)[50,51], likely reduces interspecific competition and allows for increased population sizes and carrying capacity. Given these factors, the present-day differences in effective population sizes of cutlassfish suggest a close correlation to the primary productivity differences in the East China Sea and northern South China Sea.

The historical sizes of *T. japonicus* populations in the East China Sea and northern South China Sea during the period of original coalescence and first growth peaks are comparable (Fig. 4), suggesting similar carrying capacities for these two regions prior to 45 kya. This finding is supported by the geological history of the East China Sea and northern South China Sea during the Pleistocene, specifically the wide continental shelf subsidence 150 kya[18,52] (Supplementary information S2). Given their habitat dependence on the continental shelf[24], the narrow continental shelves of the East China Sea and northern South China Sea prior to 150 kya would have provided limited habitat and supported similar population sizes of cutlassfish observed here.

The similar population sizes of *T. japonicus* observed in the East China Sea and northern South China Sea 45–150 kya (Fig. 4) are surprising given the formation of the wider East China Sea continental shelf ~150 kya[52]. Given that present population size is closely correlated to primary productivity, this finding suggests that carrying

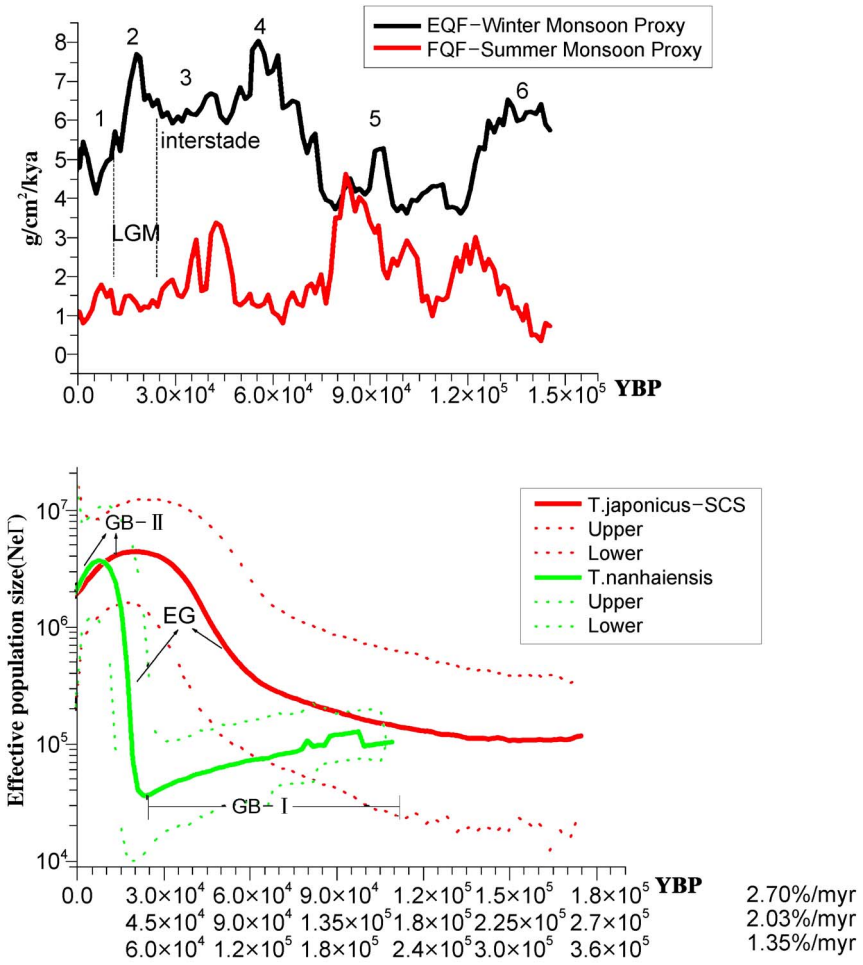

Figure 5 | History of monsoons and population dynamics of *T. nanhaiensis* and *T. japonicus* in the northern South China Sea over the past 165 kya (2.03% per myr). Top panel: East Asian monsoon changes recovered from aeolian quartz flux (EQF) and fluvial quartz flux (FQF) of Lake Biwa[55]. Bottom panel: BSPs of *T. nanhaiensis* and *T. japonicus* in the northern South China Sea. Abbreviations (EG and GB) were defined for figure 4.

capacities and levels of primary productivity between the East China Sea and northern South China Sea during this period were comparable. In terms of primary productivity, temperate rivers are thought to play more important roles than tropical rivers by contributing terrigenous organic matter and nutrients into these marginal seas (Supplementary information S3). In this context, the Changjiang contributes over 90% of river-derived runoff and particles into the East China Sea[53] and has likely had a large impact on the historical primary productivity of the East China Sea[19]. However, the geologic history of the Changjiang development during the late Pleistocene is unclear (Supplementary information S4).

If the Changjiang has drained into the East China Sea since the late Pleistocene, differences between the *T. japonicus* population sizes in the East China Sea and northern South China Sea during the last interglaciation (70–140 kya) or interstadial period (30–60 kya) should be similar to those of the present, given the increased primary productivity of the East China Sea[19] and the reduced primary productivity of the northern South China Sea[54] induced by strong summer monsoons and weak winter monsoons[55,56] (Fig. 5). However, this model is not supported by our data.

The slight glacial bottleneck observed in *T. japonicus* from the East China Sea is also indicative of the Changjiang history. During the LGM (22.5–30 kya), the sea level fell by 150 m in the East China Sea[57,58], greatly reducing the sea surface area and exposing much of the continental shelf (Fig. 1). If the Changjiang had flowed into the East China Sea prior to the LGM, freshwater and terrigenous matter flux would have greatly declined due to the reduced annual runoff from the lower Changjiang drainage by intense dry and cold winter monsoons (Fig. 5). With less nutrient input from the Changjiang, primary productivity in the East China Sea would have greatly dropped during the LGM. Subsequently, a severe population bottleneck for *T. japonicus* relative to earlier population sizes would have been expected due to losses of primary productivity and habitat size in the East China Sea. However, this is not true based on the observed slight bottleneck during the LGM (Fig. 4), suggesting a limited decrease in the primary productivity of the East China Sea during the LGM relative to that prior to the LGM and supporting the idea that the Changjiang did not historically drain into the East China Sea until the postglaciation and Holocene periods.

The recent abrupt population growth (over a 10-fold increase) observed in the East China Sea population of *T. japonicus* during 0–22.5 kya [0–15 kya for 2.7% per myr, 0–30 kya for 1.35% per myr] (Fig. 4) lends support to the hypothesis that the drainage of the Changjiang shifted to the East China Sea during the postglaciation-Holocene and increased primary productivity. Evidence from sediments of the Changjiang Delta also supports this hypothesis[59–61]. The geologic history of the Changjiang Delta can only be traced back to the late Pleistocene (MIS 3)[59] or Holocene[60,61]. Therefore, runoff from the Changjiang could not have contributed a significant amount of organic matter to the East China Sea until sea levels rose during the postglaciation or Holocene period[61], suggesting that the earlier primary productivity of the East China Sea was similar to that of the northern South China Sea. Based on these patterns, it appears that the demographic history of *T. japonicus* in the East China Sea

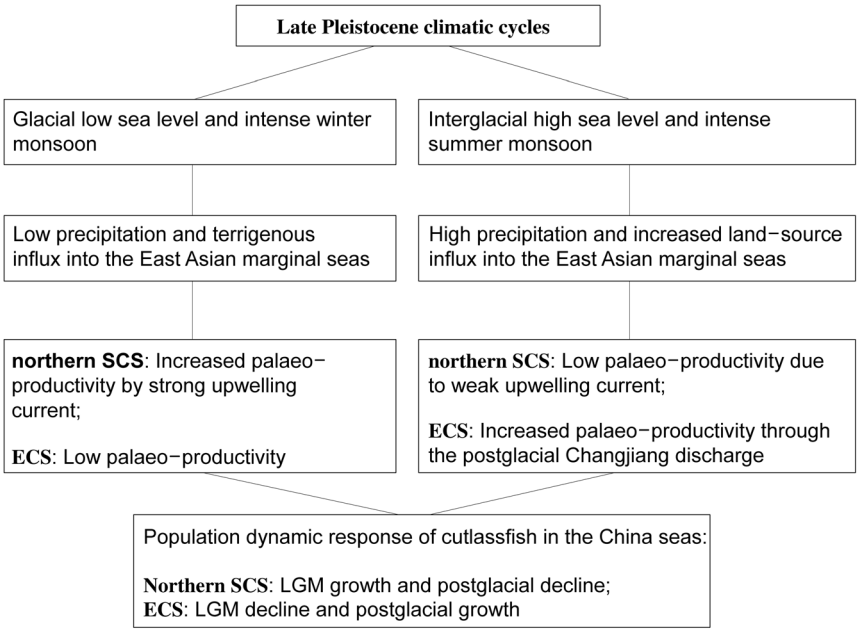

Figure 6 | Correlation of climatic changes with the palaeo-productivity and population dynamics of cutlassfish in the China seas. In the East China Sea, increased precipitation and discharge from the Changjiang during the intensified summer monsoons caused an increase in primary production. However, in the northern South China Sea, primary production was mainly influenced by nutrient advection caused by upwelling currents during winter monsoons. Thus, different population dynamic responses to climatic cycles were observed between the East China Sea and the northern South China Sea.

closely reflects the historical changes in the drainage of the Changjiang into the East China Sea since the LGM.

Compared with the glacial bottleneck and recent rapid population expansion revealed for the East China Sea population of *T. japonicus*, both the *T. japonicus* and *T. nanhaiensis* populations from the northern South China Sea exhibited a pattern of glacial growth and postglacial-Holocene decline in population size (Figs. 4, 5). Contrasting demographic patterns have also been revealed for regional populations of European *Nassarius nitidus* between two glacial refugia: an unaffected slow exponential growth in the Adriatic population during the LGM and a dramatic exponential growth after LGM in the Iberian Atlantic population[62]. The unique oceanographic and ecological conditions (*e.g.*, strong interspecific competition due to high species diversity[50], fishing pressures and changing primary productivity) may all have had dramatic impacts on the population sizes in the northern South China Sea.

However, the stress of increased competition appears not to have caused synchronous interspecific bottlenecks during the postglaciation-Holocene. While the northern South China Sea population of *T. japonicus* experienced continuous population expansion during 45–165 kya, the population of *T. nanhaiensis* steadily declined (Fig. 5, Supplementary information S5). Despite the increased catch production of the past few decades[27], no similar population bottleneck has been detected for *T. japonicus* in the East China Sea (Fig. 4). Furthermore, cutlassfish are not an economically important species in the northern South China Sea, and their catch productions exhibit a fluctuating cycle of ca. 10 years[63], suggesting that fishing pressure has also not played an important role in influencing population dynamics of cutlassfish.

The close correlation between present-day effective population sizes and primary productivity suggests that the historic palaeo-productivity along the northern slope of the South China Sea may be responsible for the similar glacial growth and postglacial/Holocene genetic bottlenecks exhibited by *T. japonicus and T. nanhaiensis*. In the northern South China Sea, primary productivity was historically mainly influenced by fluctuating winter monsoons[54] (Supplementary information S6). The peak population size of *T. japonicus* and the rapid expansion of *T. nanhaiensis* 22.5–30 kya coincide with these palaeo-productivity increases of the LGM. The subsequent rising sea levels of the postglacial period and weakened winter monsoons could have caused a population decline in *T. japonicus*. The contraction of *T. japonicus* coupled with the rising sea level of the South China Sea would have temporarily provided new niche space for *T. nanhaiensis*, leading to the continued expansion of *T. nanhaiensis* 15–22.5 kya. However, the *T. nanhaiensis* population also declined, limited by decreasing palaeo-productivity during the postglaciation-Holocene (0–15 kya)[64]. In this context, the similar glacial population growth and postglacial genetic bottlenecks experienced by *T. japonicus* and *T. nanhaiensis* in the northern South China Sea appear to indicate general responses to the palaeo-productivity history of the South China Sea during the postglacial stage and Holocene. Similar concordant responses of interspecific genetic bottlenecks to range-size constraints caused by Mid-Quaternary glaciation (0.6–1.1 Ma) were also observed in two Patagonian fish (*Galaxias maculatus* and *G. platei*)[65].

In summary, the use of BSP analyses and a calibrated *Cyt b* molecular clock of 2.03% per myr revealed a close correlation between Pleistocene glacial cycles, primary production and population dynamics of cutlassfish in the China seas. The early synchronous population growth of *T. japonicus* in both the East China Sea and the northern South China Sea likely indicates similar oceanographic conditions prior to 45 kya. However, the recent intraspecific or interspecific demographic differences of *T. japonicus* and *T. nanhaiensis* may reflect different evolutionary responses to differences in regional primary productivities induced by palaeo-hydrology and East Asian monsoon changes between the East China Sea and the northern South China Sea (Fig. 6, Supplementary information S7). Therefore, our study suggests the likelihood of genetic signs of Pleistocene climatic cycles and the postglacial development of the Changjiang Delta. A small number of similar studies regarding the dynamic response of different populations to regional environmental conditions have been conducted to date (*e.g.*, European marine Gastropoda[62], Patagonian freshwater fish[4] and humans[2]). However, future comparative studies on a wider scale regarding the evolution-

ary dynamics of marine taxa from different ecoregions are needed because they may provide additional information into past palaeoclimatic and oceanographic conditions.

Methods

Sampling and data collection. Specimens of *T. japonicus* and *T. nanhaiensis* were sampled from 11 fishing ports along the coast of the northern South China Sea (sampling sites 1–11, Fig. 1). Additional specimens of *T. japonicus* were sampled from 14 offshore stations in the East China Sea and one coastal fishing port in Xiamen, Fujian (sampling sites 12–26, Fig. 1). Muscle tissue samples from tail clips (~10 cm) were preserved in 95% ethanol for genetic analyses. Total genomic DNA was extracted from each individual using a standard phenol/chloroform approach as outlined in Sambrook *et al.*[66]. Approximately 10–30 ng of DNA was utilised as a template to amplify the full-length mitochondrial *Cyt b* gene (ca. 1200 bp) via polymerase chain reaction (PCR). Amplifications were conducted in 25 μL volumes containing 5 μL of template DNA, 1 × PCR reaction buffer, 2 mM $MgCl_2$, 300 nM each of primers CytbF and CytbR[67], 200 μM dNTPs, 0.5 unit of Taq polymerase and ddH_2O. Reactions were conducted under the following PCR conditions: an initial denaturation at 94°C for 3 min, followed by 35 cycles of 94°C for 30 s, 59°C for 60 s, 72°C for 70 s, and a final extension of 72°C for 10 min. PCR products were separated on a 1.5% agarose gel and purified with the Gel Extraction Mini Kit (Watson BioTechnologies, Shanghai, China). Purified products were sequenced in both directions using the primers pair CytbF and CytbR on an ABI Prism 3730 automatic sequencer.

Data analyses. *Genetic diversity and haplotype networks.* *Cyt b* gene sequences were aligned using Clustal_X[68] under default parameters, and the quality of the alignments was checked through the correct translation at the amino acid level. To confirm species identification, sequenced haplotypes were compared with *T. japonicus* (DQ364150) and *T. nanhaiensis* (JX477078) sequences from GenBank.

To visualise relationships among *Cyt b* haplotypes, intraspecific median-joining networks[69] were constructed for each species using NETWORK version 4.6.1.0 (Fluxus Engineering, 2012). To avoid hyperlinks and complex reticulations between haplotypes, the weight of hypervariable sites (number of mutations > 12) were set to 0, and the weights of other variable sites were proportionally adjusted according to their mutation frequencies (e.g., the weights of minimum mutation events (number of mutations = 1) were increased to 90, and the weight of sites with 10 mutations was downweighted to 9).

To reveal the regional responses of *T. japonicus* to different oceanographic conditions, the *T. japonicus* data set was divided into two geographic groups corresponding to two main marine ecosystems/ecoregions: the northern South China Sea and the East China Sea. Though these seas connect through the Taiwan Strait, they possess different biogeochemical properties and species assemblages[23,70] and can be divided near the southern tip of Taiwan Island and Dongshan of Fujian province (dashed line in Fig. 1). Nucleotide (π) and haplotype (h) diversity estimates were calculated for each species, sampling site and geographic group according to the methods of Nei[71] using ARLEQUIN[72] (version 3.5).

Molecular rate calibration. DNA calibration methods based on fossil data and ancient geologic events (*i.e.*, >1 Mya) have been shown to be unreliable and to underestimate evolutionary rates at the population level[40,41,73]. However, several recent geological and climatic events may serve as possible calibration points for the evolution of cutlassfish in the China seas: (1) the formation of the wide continental shelf of the East China Sea ~ 150 kya, when coastal East China subsided during the last uplift of the Tibetan Plateau[18]; (2) the flooding of the newly formed East China Sea shelf during sea level highstands of the Last Interglaciation (70–140 kya)[74]; and (3) the postglaciation-Holocene (0–22 kya) flooding of the East China Sea shelf as sea levels rose again after the Last Glacial exposure. Given the dependence of cutlassfish on continental shelf for habitat[24], the newly formed wide East China Sea shelf and its subsequent flooding 70–140 kya likely prompted the earliest period of population expansion for cutlassfish in the East China Sea. Thus, an approximate molecular clock for *Trichiurus* was inferred from the population expansion parameter τ ($\tau = 2ut$; where t measures time in generations, τ measures time in units of 1/2u generations, and u is the mutation rate of the entire region of DNA under study)[29]; where t = 70–140 kyr and τ ($\tau = 4.289$) is estimated from the mismatch distribution analyses in ARLEQUIN. The mutation rate parameter, u, was estimated from the equation $u = m\mu$, where m is the fragment length (m = 1127 for *Cyt b*) and μ is the within-lineage mutation rate per nucleotide.

Demographic history. Historical demographic patterns for each species and for the two geographic groups of *T. japonicus* (northern South China Sea and East China Sea) were investigated in ARLEQUIN using the mismatch distribution of pairwise nucleotide differences between haplotypes. Populations that have experienced recent demographic expansions are expected to exhibit a unimodal mismatch distribution, whereas a multi-modal distribution is expected for populations in genetic equilibrium[29,75]. Furthermore, two neutrality tests, Tajima's D[76] and Fu's F_s[77] were used to infer past population dynamics. Both methods provide information regarding demographic history in the absence of selection, with significant negative or positive values generally suggesting population expansions or bottlenecks[76–78], respectively.

To compare complex Skyline-Plot models against constant demographic models, extended Bayesian Skyline Plots (EBSPs)[79] were run to estimate the number of changes present in each data set. The demographic histories of *T. japonicus* and *T. nanhaiensis* were further investigated using a coalescent-based BSP model with a Markov Chain Monte Carlo (MCMC) sampling procedure in BEAST v 1.7.4[80] under a strict molecular clock, 2.03% (1.35%–2.7%) per myr. Three independent runs were combined using LogCombiner and visualised in TRACER[81]. The MCMC analysis was run for over 6×10^8 generations to ensure a high effective sample size (ESS: >200), of which the first 10% was discarded as burn-in. The evolutionary model of each data set was estimated using Modeltest 3.7[82].

1. Hewitt, G. M. Post-glacial re-colonization of European biota. *Biol. J. Linn. Soc.* **68**, 87–112 (1999).
2. Atkinson, Q. D., Gray, R. D. & Drummond, A. J. mtDNA Variation predicts population size in humans and reveals a major southern Asian chapter in human prehistory. *Mol. Biol. Evol.* **25**, 468–474 (2008).
3. Gratton, P., Konopiński, M. K. & Sbordoni, V. Pleistocene evolutionary history of the Clouded Apollo (*Parnassius mnemosyne*): genetic signatures of climate cycles and a 'time-dependent' mitochondrial substitution rate. *Mol. Ecol.* **17**, 4248–4262 (2008).
4. Ruzzante, D. E. *et al.* Climate control on ancestral population dynamics: insight from Patagonian fish phylogeography. *Mol. Ecol.* **17**, 2234–2244 (2008).
5. Jones, C. P. & Johnson, J. B. Phylogeography of the livebearer *Xenophallus umbratilis* (Teleostei: Poeciliidae): glacial cycles and sea level change predict diversification of a freshwater tropical fish. *Mol. Ecol.* **18**, 1640–1653 (2009).
6. Larmuseau, M. H. D., Van Houdt, J. K. J., Guelinckx, J., Hellemans, B. & Volckaert, F. A. M. Distributional and demographic consequences of Pleistocene climate fluctuations for a marine demersal fish in the north-eastern Atlantic. *J. Biogeogr.* **36**, 1138–1151 (2009).
7. He, L. J., Zhang, A. B., Zhu, C. D., Weese, D. & Qiao, Z. G. Phylogeography of the mud crab (*Scylla serrata*) in the Indo-West Pacific reappraised from mitochondrial molecular and oceanographic clues: Transoceanic dispersal and coastal sequential colonization. *Mar. Ecol.* **32**, 52–64 (2011).
8. Liu, J. X. *et al.* Effects of Pleistocene climatic fluctuations on the phylogeographic and demographic histories of Pacific herring (*Clupea pallasii*). *Mol. Ecol.* **20**, 3879–3893 (2011).
9. De Bruyn, M. *et al.* Rapid response of a marine mammal species to Holocene climate and habitat change. *PLoS Genet.* **5**, e1000554 (2009).
10. He, L. J. *et al.* Late Pleistocene expansion of *Scylla paramamosain* along the coast of China: a population dynamic response to the Last Interglacial sea level highstand. *J. Exp. Mar. Biol. Ecol.* **385**, 20–28 (2010).
11. Allcock, A. L. & Strugnell, J. M. Southern Ocean diversity: new paradigms from molecular ecology. *Trends Ecol. Evol.* **27**, 520–528 (2012).
12. Hopkins, D. M. The paleogeography and climatic history of Beringia during late Cenozoic time. *Int. J. Arct. Nord. Stud.* **12**, 121–150 (1972).
13. Wang, P. X. Response of Western Pacific marginal seas to glacial cycles: paleoceanographic and sedimentological features. *Mar. Geol.* **156**, 5–39 (1999).
14. Brigham-Grette, J. New perspectives on Beringian Quaternary paleogeography, stratigraphy, and glacial history. *Quat. Sci. Rev.* **20**, 15–24 (2001).
15. Hanebuth, T., Stattegger, K. & Grootes, P. M. Rapid flooding of the Sunda Shelf: a late-glacial sea-level record. *Science* **288**, 1033–1035 (2000).
16. Shapiro, B. *et al.* Rise and fall of the Beringian steppe bison. *Science* **306**, 1561–1565 (2004).
17. Yasuhara, M., Cronin, T. M., deMenocal, P. B., Okahashi, H. & Linsley, B. K. Abrupt climate change and collapse of deep-sea ecosystems. *Proc. Natl. Acad. Sci.* **105**, 1556–1560 (2008).
18. Wang, P. X. Cenozoic deformation and the history of sea-land interactions in Asia. in *Continent-Ocean Interactions in the East Asian Marginal Seas* (eds Clift, P., Wang, P. X., Kuhnt, W. & Hayes, D.). *Geophysical Monograph* **149**, 1–22 (AGU, 2004).
19. Gong, G. C. *et al.* Yangtze River floods enhance coastal ocean phytoplankton biomass and potential fish production. *Geophys. Res. Lett.* **38**, L13603 (2011).
20. Liu, J. X. *et al.* Late Pleistocene divergence and subsequent population expansion of two closely related fish species, Japanese anchovy (*Engraulis japonicus*) and Australian anchovy (*Engraulis australis*). *Mol. Phylogenet. Evol.* **40**, 712–723 (2006).
21. Iwamoto, K., Chang, C. W., Takemura, A. & Imai, H. Genetically structured population and demographic history of the goldlined spinefoot *Siganus guttatus* in the northwestern Pacific. *Fisheries Sci.* **78**, 249–257 (2012).
22. Wang, L., Shi, X. F., Su, Y. Q., Meng, Z. N. & Lin, H. R. Genetic divergence and historical demography in the endangered large yellow croaker revealed by mtDNA. *Biochem. Syst. Ecol.* **46**, 137–144 (2013).
23. Sherman, K. & Duda, A. M. An ecosystem approach to global assessment and management of coastal waters. *Mar. Ecol. Prog. Ser.* **190**, 271–287 (1999).
24. Nelson, J. S. *Fishes of the World*. 3rd edn.(John Wily & Sons, New York, 1994).
25. FAO Fishery Information, Data and Statistics Unit. *Capture production 2002, FAO yearbook*. Fishery statistics, 94/1. Rome: Food and Agricultural Organisation (FAO) (2004).
26. Cheng, J. H. & Mi, C. D. Hairtails. in *The Biological Resources and Environment in Continental Shelf of the East China Sea*. (eds Zhen, Y. J. *et al.*) 450–472 (Shanghai Science and Technology Press, Shanghai, 2003).
27. Mi, C. D. A study on resources, stock structure and variation of reproductive habit of hairtail *Trichiurus haumela* in East China Sea. *J. Fish. Sci. China* **4**, 7–14 (1997).

28. Zhou, Y. D., Xu, H. X., Liu, Z. F. & Xue, L. J. A study on variation of stock structure of hairtail *Trichiurus haumela* in the East China Sea. *J. Zhejiang Ocean. Univ. (Nat Sci)* **21**, 314–320 (2002).
29. Rogers, A. R. & Harpending, H. Population growth makes waves in the distribution of pairwise genetic differences. *Mol. Biol. Evol.* **9**, 552–569 (1992).
30. Drummond, A. J., Rambaut, A., Shapiro, B. & Pybus, O. G. Bayesian coalescent inference of past population dynamics from molecular sequences. *Mol. Biol. Evol.* **22**, 1185–1192 (2005).
31. Xu, J. W., Chan, T. Y., Tsang, L. M. & Chu, K. H. Phylogeography of the mitten crab *Eriocheir sensu stricto* in East Asia: Pleistocene isolation, population expansion and secondary contact. *Mol. Phylogenet. Evol.* **52**, 45–56 (2009).
32. Hoffman, J. I., Grant, S. M., Forcada, J. & Phillips, C. D. Bayesian inference of a historical bottleneck in a heavily exploited marine mammal. *Mol. Ecol.* **20**, 3989–4008 (2011).
33. Bowen, B. W., Muss, A., Rocha, L. A. & Grant, W. S. Shallow mtDNA coalescence in Atlantic pygmy angelfishes (Genus *Centropyge*) indicates a recent invasion from the Indian Ocean. *J. Hered.* **97**, 1–12 (2006).
34. McMillan, W. O. & Palumbi, S. R. Rapid rate of control-region evolution in butterflyfishes. *J. Mol. Evol.* **45**, 473–484 (1997).
35. Doadrio, I. & Perdices, A. Phylogenetic relationships among the Ibero-African cobitids (*Cobitis*, Cobitidae) based on cytochrome *b* sequence data. *Mol. Phylogenet. Evol.* **37**, 484–493 (2005).
36. Dowling, T. E., Tibbets, C. A., Minckley, W. L. & Smith, G. R. Evolutionary relationships of the plagopterins (Teleostei: Cyprinidae) from cytochrome *b* sequences. *Copeia* **2002**, 665–678 (2002).
37. Tsigenopoulos, C. S., Durand, J. D., Ünlü, E. & Berrebi, P. Rapid radiation of the Mediterranean *Luciobarbus* species (Cyprinidae) after the Messinian salinity crisis of the Mediterranean Sea, inferred from mitochondrial phylogenetic analysis. *Biol. J. Linn. Soc.* **80**, 207–222 (2003).
38. Martin, A. & Bermingham, E. Systematics and evolution of lower Central American cichlids inferred from analysis of cytochrome *b* gene sequences. *Mol. Phylogenet. Evol.* **9**, 192–203 (1998).
39. He, D. K., Chen, Y. F., Chen, Y. Y. & Chen, Z. M. Molecular phylogeny of the specialized schizothoracine fishes (Teleostei: Cyprinidae), with their implications for the uplift of the Qinghai-Tibetan Plateau. *Chin. Sci. Bull.* **49**, 39–48 (2004).
40. Ho, S. Y. W., Phillips, M. J., Cooper, A. & Drummond, A. J. Time dependency of molecular rate estimates and systematic overestimation of recent divergence times. *Mol. Biol. Evol.* **22**, 1561–1568 (2005).
41. Burridge, C. P., Craw, D., Fletcher, D. & Waters, J. M. Geological dates and molecular rates: fish DNA sheds light on time dependency. *Mol. Biol. Evol.* **25**, 624–633 (2008).
42. Santos, C. *et al*. Understanding differences between phylogenetic and pedigree-derived mtDNA mutation rate: a model using families from the Azores Islands (Portugal). *Mol. Biol. Evol.* **22**, 1490–1505 (2005).
43. Kemp, B. M. *et al*. Genetic analysis of early Holocene skeletal remains from Alaska and its implications for the settlement of the Americas. *Am. J. Phys. Anthropol.* **132**, 605–621 (2007).
44. Crandall, E. D., Sbrocco, E. J., DeBoer, T. S., Barber, P. H. & Carpenter, K. E. Expansion dating: calibrating molecular clocks in marine species from expansions onto the Sunda Shelf following the Last Glacial Maximum. *Mol. Biol. Evol.* **29**, 707–719 (2012).
45. Finney, B. P., Gregory-Eaves, I., Douglas, M. S. V. & Smol, J. P. Fisheries productivity in the northeastern Pacific Ocean over the past 2, 200 years. *Nature* **416**, 729–733 (2002).
46. Beaugrand, G. & Reid, P. C. Long-term changes in phytoplankton, zooplankton and salmon related to climate. *Global Change Biol.* **9**, 801–817 (2003).
47. Schaaf, A. Sea level changes, continental shelf morphology, and global paleoecological constraints in the shallow benthic realm: a theoretical approach. *Palaeogeogr. Palaeoclimatol. Palaeoecol.* **121**, 259–271 (1996).
48. Tan, S. C. & Shi, G. Y. Satellite-derived primary productivity and its spatial and temporal variability in the China seas. *J. Geogr. Sci.* **16**, 447–457 (2006).
49. Pauly, D. & Christensen, V. Primary production required to sustain global fisheries. *Nature* **374**, 255–279 (1995).
50. Huang, Z. G. General characteristics of species in China seas. *Chin. Biodivers.* **2**, 63–67 (1994).
51. Chen, Q. C. Current status and prospects of marine biodiversity in China. *Chin. Biodivers.* **5**, 142–146 (1997).
52. Sun, X. J., Luo, Y. L., Huang, F., Tian, J. & Wang, P. X. Deep-sea pollen from the South China Sea: Pleistocene indicators of East Asian monsoon. *Mar. Geol.* **201**, 97–118 (2003).
53. Wang, P. X. *et al. Foraminifera and Ostracods in Bottom Sediment of the East China Sea*. (China Ocean Press, Beijing, 1988).
54. Wang, R. J. *et al*. Quaternary biogenic opal records in the South China Sea: linkages to East Asian monsoon, global ice volume and orbital forcing. *Sci. China Earth Sci.* **50**, 710–724 (2007).
55. Xiao, J. L. *et al*. East Asian monsoon variation during the last 130,000 years: Evidence from the Loess Plateau of central China and Lake Biwa of Japan. *Quat. Sci. Rev.* **18**, 147–157 (1999).
56. Shi, Y. F. & Zhao, J. D. The special warm-humid climate and environment in China during 40 ~ 30 ka BP: Discovery and review. *J. Glaciol. Geocryol.* **31**, 1–10 (2009).
57. Zhu, Y. Q., Li, C. Y., Zeng, C. K. & Li, B. G. The lowest sea level on the East China Sea shelf during the late Pleistocene. *Chin. Sci. Bull.* **24**, 317–320 (1979).
58. Feng, Y. J. Sea level changes and the lowest sea level in the East China Sea since 40,000 years. *Donghai Mar. Sci.* **1**, 36–42 (1983).
59. Li, C. X., Chen, Q. Q., Zhang, J. Q., Yang, S. Y. & Fan, D. D. Stratigraphy and paleoenvironmental changes in the Yangtze Delta during the Late Quaternary. *J. Asian Earth Sci.* **18**, 453–469 (2000).
60. Hori, K., Saito, Y., Zhao, Q. H. & Wang, P. X. Architecture and evolution of the tide-dominated Changjiang (Yangtze) River delta, China. *Sediment. Geol.* **146**, 249–264 (2002).
61. Liu, J. P. *et al*. Flux and fate of Yangtze River sediment delivered to the East China Sea. *Geomorphology* **85**, 208–224 (2007).
62. Albaina, N., Olsen, J. L., Couceiro, L., Ruiz, J. M. & Barreiro, R. Recent history of the European *Nassarius nitidus* (Gastropoda): phylogeographic evidence of glacial refugia and colonization pathways. *Mar. Biol.* **159**, 1871–1884 (2012).
63. Lu, W. H. Fishing Catch from bottom trawls along the coast of Guangdong province. In *The Second Session of the Dongguan City Youth Science and Technology Symposium*. (eds Dongguan Association of science and technology) 71–76 (Guangdong, China, 2001).
64. Li, J. & Wang, R. J. Paleoproductivity variability of the northern South China Sea during the past 1 Ma: The opal record from ODP site 1144. *Acta Geol. Sin.* **78**, 228–233 (2004).
65. Zemlak, T. S., Walde, S. J., Habit, E. M. & Ruzzante, D. E. Climate-induced changes to the ancestral population size of two Patagonian galaxiids: the influence of glacial cycling. *Mol. Ecol.* **20**, 5280–5294 (2011).
66. Sambrook, J., Fritsch, E. F. & Maniatis, T. *Molecular Cloning: A laboratory Manual*. 2nd edn (Cold Spring Harbor Laboratory, New York, 1989).
67. Tzeng, C. H., Chen, C. S. & Chiu, T. S. Analysis of morphometry and mitochondrial DNA sequences from two *Trichiurus* species in waters of the western North Pacific: taxonomic assessment and population structure. *J. Fish. Biol.* **70** (Suppl. B), 165–176 (2007).
68. Thompson, J. D., Gibson, T. J., Plewniak, F., Jeanmougin, F. & Higgins, D. G. The ClustalX windows interface: flexible strategies for multiple sequence alignment aided by quality analysis tools. *Nucleic Acids Res.* **25**, 4876–4882 (1997).
69. Bandelt, H. J., Forster, P. & Röhl, A. Median-joining networks for inferring intraspecific phylogenies. *Mol. Biol. Evol.* **16**, 37–48 (1999).
70. Spalding, M. D. *et al*. Marine ecoregions of the world: A bioregionalization of coastal and shelf areas. *Bioscience* **57**, 573–593 (2007).
71. Nei, M. *Molecular Evolutionary Genetics*. (Columbia University Press, New York, 1987).
72. Excoffier, L. & Lischer, H. E. L. Arlequin suite ver 3.5: A new series of programs to perform population genetics analyses under Linux and Windows. *Mol. Ecol. Resour.* **10**, 564–567 (2010).
73. Ho, S. Y. W. & Larson, G. Molecular clocks: When times are a-changin. *Trends Genet.* **22**, 79–83 (2006).
74. Winograd, I. J., Landwehr, J. M., Ludwig, K. R., Coplen, T. B. & Riggs, A. C. Duration and structure of the past four interglaciations. *Quatern. Res.* **48**, 141–154 (1997).
75. Harpending, H. C. Signature of ancient population growth in a low-resolution mitochondrial-DNA mismatch distribution. *Hum. Biol.* **66**, 591–600 (1994).
76. Tajima, F. The effect of change in population-size on DNA polymorphism. *Genetics* **123**, 597–601 (1989).
77. Fu, Y. X. Statistical tests of neutrality of mutations against population growth, hitchhiking and background selection. *Genetics* **147**, 915–925 (1997).
78. Akey, J. M. *et al*. Population history and natural selection shape patterns of genetic variation in 132 genes. *PLoS Biol.* **2**, e286 (2004).
79. Heled, J. & Drummond, A. J. Bayesian inference of population size history from multiple loci. *BMC Evol. Biol.* **8**, 289 (2008).
80. Drummond, A. J. & Rambaut, A. BEAST: Bayesian evolutionary analysis by sampling trees. *BMC Evol. Biol.* **7**, 214 (2007).
81. Rambaut, A., Suchard, M. & Drummond, A. J. Tracer v1.6. Available from http://tree.bio.ed.ac.uk/software/tracer/ (2013) Date of access: 11/12/2013.
82. Posada, D. & Crandall, K. A. MODELTEST: testing the model of DNA substitution. *Bioinformatics* **14**, 817–818 (1998).
83. Waelbroeck, C. *et al*. Sea-level and deep water temperature changes derived from benthic foraminifera isotopic records. *Quat. Sci. Rev.* **21**, 295–305 (2002).

Acknowledgments

Kind help was provided for collecting field samples in the East China Sea and South China Sea by JH Cheng, LP Yan, and CQ Fan. Helpful comments for improving the original manuscript were provided by XY Wu, B Deng and J Hu. This study was funded by the National Natural Science Foundation of China (Grant No. 30800117), the Key Project of Chinese National Programs for Fundamental Research and Development (973 Program) (No. 2011CB409801) and the State Key Laboratory of Estuarine and Coastal Research, East China Normal University (No. SKLEC-2012KYYW05).

Author contributions

L.J.H. performed study design, field sampling, laboratory work, data analysis and manuscript preparation, A.B.Z. and D.W. contributed to the data analysis, manuscript

editing and discussion, S.F.L. and J.S.L. helped with sampling from the East China Sea, and J.Z. helped with sampling in the South China Sea and contributed to editing and improving this manuscript.

Additional information

Accession Codes: DNA sequences: accessions KF551253–KF551565 in GenBank.

Supplementary information accompanies this paper at http://www.nature.com/scientificreports

Competing financial interests: The authors declare no competing financial interests.

How to cite this article: He, L. *et al.* Demographic response of cutlassfish (*Trichiurus japonicus and T. nanhaiensis*) to fluctuating palaeo-climate and regional oceanographic conditions in the China seas. *Sci. Rep.* **4**, 6380; DOI:10.1038/srep06380 (2014).